PII: S0143-7208(96)00067-8

ELSEVIER

Immersional Wetting of Zirconium Silicate Surfaces

P. A. Chan,[a] J. T. Guthrie[a] & P. J. Smith[b]

[a]The Department of Colour Chemistry and Dyeing, The University of Leeds,
Leeds LS2 9JT, U.K.
[b]Cookson Technology Centre, Oxford OX5 1PF, U.K.

ABSTRACT

The heats of immersion of various grades of zirconium silicate (zircon) pow-
der have been measured in water. The sub-divided samples had specific surface
areas in the range 1.60 m^2 g^{-1} to 11.10 m^2 g^{-1}. The powders were degassed
on a vacuum line for several hours prior to measurement. The heats of surface
hydration were found to be between 0.17 kJ mol^{-1} and 0.70 kJ mol^{-1}. The
increase in the heats of immersion corresponds to a decrease in the coarseness
of the powder and an increase in the specific surface area. © 1997 Elsevier
Science Ltd

Keywords: heats of immersion, zircon, zirconium silicate, heats of surface
hydration, wetting, colorimetry.

INTRODUCTION

The mineral zirconium silicate (zircon, $ZrSiO_4$)[1] has been known as a
gemstone since the middle ages. It occurs mainly within granites and syne-
nites in many widely separated locations.

Zircon is chemically very stable, especially at low temperatures. It is gen-
erally insoluble in mineral acids, the exception being the slight solubility
which occurs in hydrofluoric acid. Physically, zircon possesses a high refrac-
tivity. It has no definite melting point but, at temperatures above 1550°C,
zircon begins to dissociate into zirconia and silica. The refractive index of
zircon is ≈2.0. It is similar to that of tin oxide and antimony trioxide, but
less than that of titanium dioxide (rutile), which has a refractive index value
of 2.7. Due to its chemical and physical properties, zircon has found

considerable use in the ceramics industry as a refractory and an opacifying material.

When a cleaved crystal surface is wetted by a liquid, heat is generated. This phenomenon has been known since the report by Pouillet ('The Pouillet Effect') in 1822 [2]. Other terms used to define this effect are heat of wetting [3] and the heats of immersion. Boyd and Harkins [4] used the term 'heat of emersion' to refer to the reverse thermal process, namely that of stripping the liquid off the solid to leave a clean surface. In the 1930s calorimeters of reasonable quality were being developed to measure this level of heat exchange. Attention was also given to outgassing techniques, prior to immersion. A large number of experimental results on the heats of wetting of various systems was obtained by different investigators. Few of these, however, carry a significant level of reliability, due to the lack of information regarding the state and purity of the solid surfaces and the paucity of data concerning the liquids used in the wetting experiments. Contamination of the powders before immersion caused by adsorbed films of water, was also a major source of error seen in earlier work and resulted in a reduced amount of heat being evolved [4].

Boyd and Harkins [4] showed that, for a range of metal oxides, the heat of evolution was caused by a change in the interfacial energies alone. This was demonstrated by two simple experiments. In the first, it was found that for the same solid in two or more states of subdivision, the heat change was directly proportional to the surface area. In the second, it was shown that when various amounts of the same powder were used, the heat evolved was directly proportional to the mass of powder. Their study is considered to be important because care was taken regarding the special problems of immersional calorimetry. Thus, surface areas were obtained (Brunauer–Emmett–Teller adsorption isotherm; BET), providing a means of placing measured exothermicity data on a unit area basis. The heat output was measured using a 36-junction thermocouple and a double potentiometer with a sensitive galvanometer [5].

Early investigators used Beckmann thermometers for the measurement of small heat changes. However, these thermometers have the disadvantages of possessing large thermal capacity and a slow response to small temperature changes. Boyd and Harkins overcame these difficulties. However, considerable precautions had to be taken to prevent the pick-up of spurious signals leading to inaccuracies. In 1946, Hutchinson [6] developed a method of accurate thermometry which fulfilled all the requirements of accuracy and responsiveness and, in addition, was very compact and easy to operate. He used a 'thermistor' (resistance thermometer) composed of a mixture of fused oxides, principally uranium oxide, sealed by means of thin platinum wires, in a protective sleeve.

During this period, thermistors were the subject of considerable research [7]. Hutchinson appears to have been the first to use a thermistor in the accurate determination of small temperature rises. Zettlemoyer *et al.* [8] later provided a detailed study of the use of a thermistor, which was connected to a Mueller bridge, as the temperature sensing element. This was later expanded to twin calorimetry by Bartell and Suggit [3], through use of two thermistors: in opposite arms of a Wheatstone bridge with a double potentiometer across the bridge. Thermistor calorimeters have since gained wide use because of the simple construction and operation [9–11].

In this study, heats of immersion have been measured using a calibrated thermistor calorimeter. Prior to the measurements, an exhaustive, reproducible cleaning regime was performed on the powders.

This approach has been adopted to determine the surface characteristics of zircon powders. Such studies are of relevance to the ceramics industry, as very little literature is available on the fundamental surface characteristics of zircon.

EXPERIMENTAL

Materials

The zircon samples in four states of subdivision were obtained from Cookson Matthey Ceramics and Minerals (Cookson House, Willington Quay Wallsend, Tyne and Wear, UK). The samples originated from the same source to ensure greater consistency of composition.

The water used in this study was distilled on an Elga distillation unit (Elga Ltd, Lane End, High Wycombe, Bucks, UK). This unit works on a reverse osmosis principle.

The as-received powders were sieved using a 45 μm sieve. Prior to the heats of immersion measurements, a comprehensive physical characterisation of the powders was carried out. This involved determination of the specific surface area (BET), particle size (Malvern Mastersizer and Coulter Counter), porosity (mercury intrusion porosimetry) and surface morphology (scanning electron microscopy; SEM). The powders were also degassed on the vacuum unit for several hours, using a freeze/thaw method, before thermal sealing under vacuum at $\sim 1 \times 10^{-4}$ mbar.

Apparatus

In developing a suitable calorimeter for measurement of the minute quantity of heat evolved when a powder is immersed in a liquid, consideration must be given to the need to ensure the provision of a steady and sufficient stirring

rate, accurate measurement of the electrical energy equivalent and sufficiently rapid attainment of thermal equilibrium [4].

In order to measure the heats of immersion two units were designed and built. The first was a high vacuum system used to clean/degas the powder surface (removing any adsorbed water, O_2 or N_2) via the freeze/thaw method. The second was an immersion unit. This was used to measure the amount of heat evolved, as the total energy of immersion, when the powder is immersed in or wetted by a liquid.

The vacuum system consists of an Edwards E02K diffusion pump working in conjunction with an Edwards E2M standard rotary pump, (Edwards High Vacuum International, Manor Royal, Crawley, West Sussex, UK). The system is capable of achieving an ultimate vacuum of $\sim 1 \times 10^{-5}$ mbar.

The sample bulbs are designed such that they have a radius of 20 mm, a wall thickness of ~ 0.5 mm and are connected to a 14 mm long, quick-fit cylindrical piece of glass tubing from which the bulb was blown. The overall layout is shown in Fig. 1.

Heats of immersion were measured at 20°C using an immersion unit as depicted in Fig. 2. This consists of a thick walled Dewar (~ 4 cm), made from poly(ethylene), with a capacity of 1 dm^3. Housed inside the vessel are a

1. Vapour diffusion pump
2. High vacuum isolation valve
3. High vacuum system
4. Water trap
5. High vacuum valve
6. High vacuum gauge head (Penning)
7. Nitrogen gas admittance valve
8. Sample bulb
9. Roughing valve
10. Air admittance valve
11. Backing valve
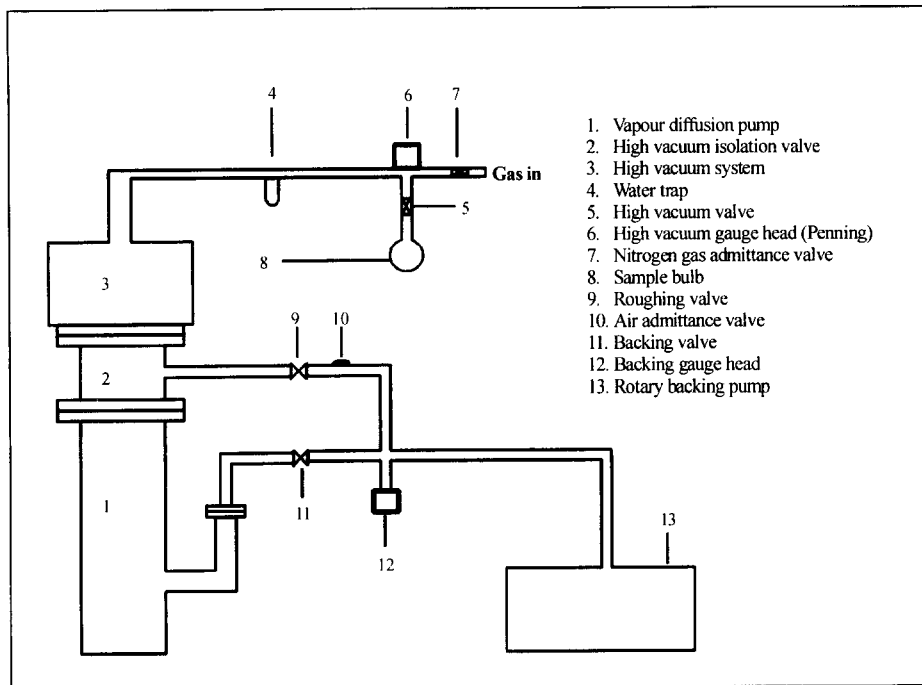12. Backing gauge head
13. Rotary backing pump

Fig. 1. The vacuum system.

sample bulb holder, an electrical heater (used in calibration of the system) and a Nylon stirring rod. The rod rotates at 420 rpm before and after the bulb is ruptured. The sample bulbs were broken by gently tapping the bulbs onto a tungsten spike.

Temperature changes were measured using 4700 Ω, bead thermistors as the sensing devices. The circuit used, shown in Fig. 3, is a classic Wheatstone bridge, with a potentiometer incorporated. The circuit is balanced when $(R_2 + R_3)/(R_4 + R_5) = (R_1/R)$. The bridge circuit works in conjunction with a high gain amplifier and is capable of measuring a response of 1562 mV per °C.

A - Sample holder
B - Electrical heater
C - Thermistor
D - Dewar
E - Sample bulb
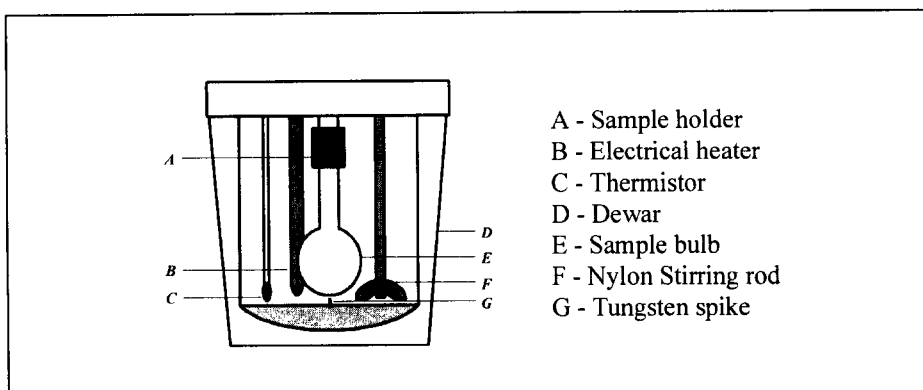F - Nylon Stirring rod
G - Tungsten spike

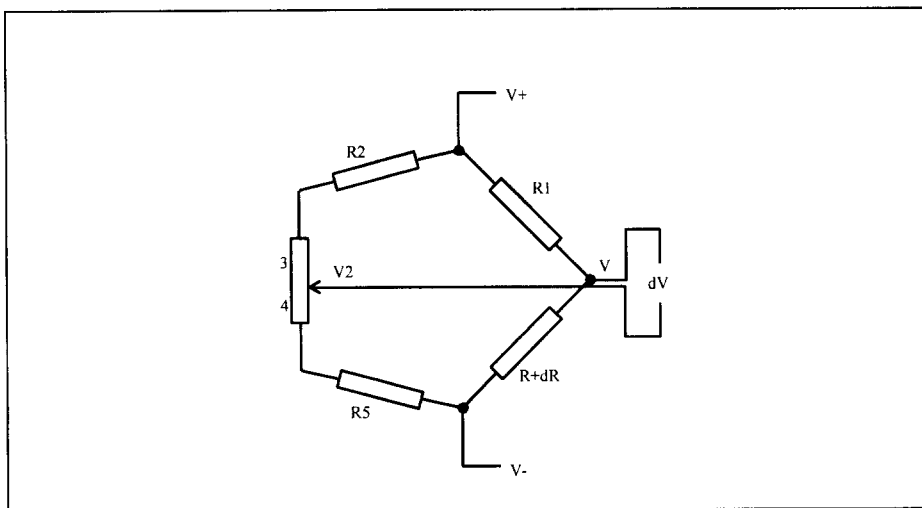**Fig. 2.** The immersion unit layout.

Fig. 3. The thermistor circuit.

Pore size distributions can be determined using mercury intrusion porosimetry [12]. The volume of mercury, which can be forced into the pores of the solid is measured as a function of the applied pressure.

The pore size distribution is calculated in accordance with the equation for the pressure difference across a curved liquid interface.

$$p = 2\gamma \cos \theta / r$$

Here γ denotes the surface tension of mercury and θ the contact angle ($\theta \approx 140°$ with most solids). Using this technique, one can determine the size and nature of void spaces and the pores in porous materials [13]. The volume of mercury that penetrates the sample is a direct measure of the voids and/or the pores within the sample, which are capable of being filled by the mercury.

RESULTS

Table 1 shows the results obtained from particle size analysis of the processed powders. The values given are an average of three measurements. The approximate drift from the mean was in the range 1–5% for the Malvern Mastersizer and for the Coulter Counter was between 1 and 7%.

Figure 4 shows the particle size distribution curves obtained from a Malvern Mastersizer. Here (A) and (B) show Zircon 1a and Zircon 2b and (C) and (D) show Zircon 3c and Zircon 4d, respectively.

TABLE 1
Particle Size Analysis

Sample	Particle D_{50} (μm)[a]	Particle D_{50} (μm)[b]
Zircon 1a	1.75	5.67
Zircon 2b	1.53	4.38
Zircon 3c	1.76	5.93
Zircon 4d	9.77	7.21

TABLE 2
Surface Area and Total Pore Area Measurements

Sample	Specific Surface Area ($m^2 \, g^{-1}$)	Total Pore Area ($m^2 \, g^{-1}$)
Zircon 1a	11.10	22.18
Zircon 2b	7.10	12.73
Zircon 3c	6.40	9.33
Zircon 4d	1.60	3.33

TABLE 3
Heat of Immersion Measurements

Sample	δH_1 (J g^{-1})	δH_1 (J m^{-2})[a]	δH_1 (J m^{-2})[b]	δH_1 (kJ mol^{-1})
Zircon 1a	3.83	0.34	0.17	0.70
Zircon 2b	2.53	0.35	0.19	0.46
Zircon 3c	2.50	0.39	0.26	0.45
Zircon 4d	0.95	0.59	0.28	0.17

[a]Values calculated from specific surface areas (BET).
[b]Values calculated from total pore areas (Mercury intrusion porosity).
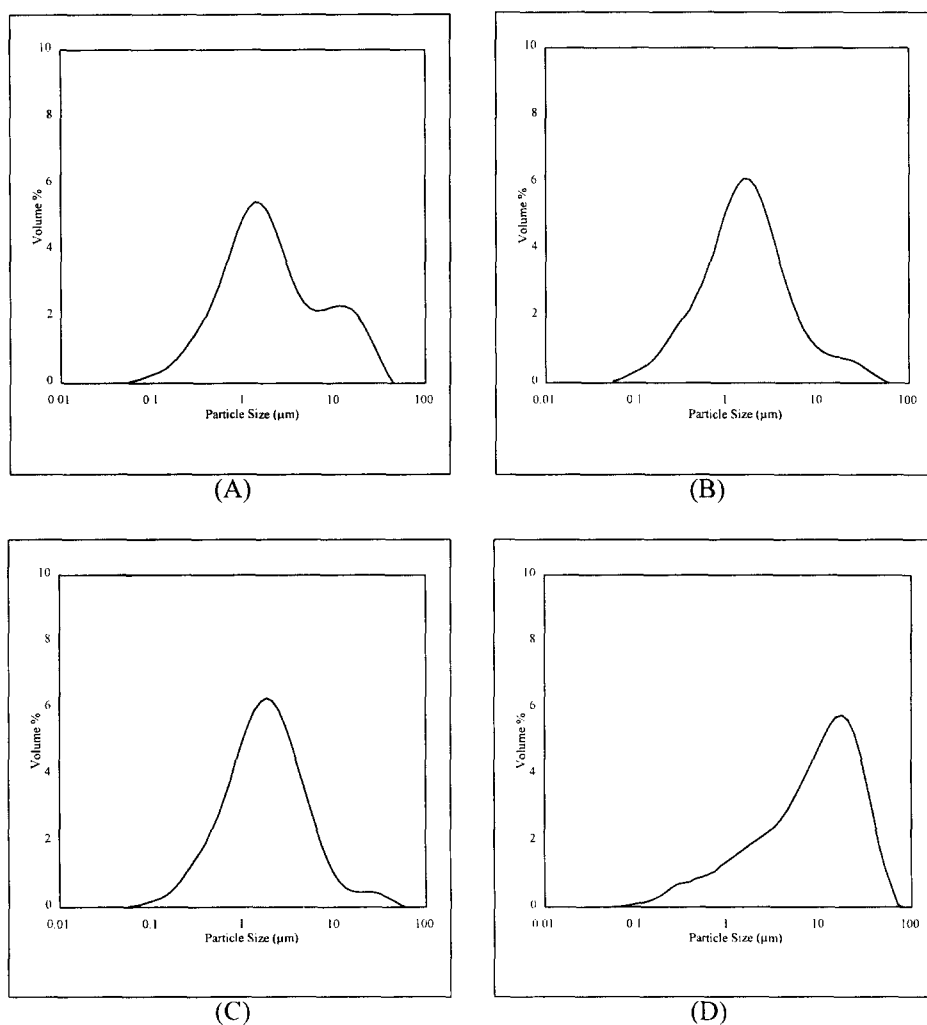
Fig. 4. Particle size distribution curves, Malvern Mastersizer.

Figure 5 shows the SEM micrographs of the four Zircon samples. Here (A), (B), (C) and (D) show Zircon 1a, Zircon 2b, Zircon 3c and Zircon 4d, respectively. It can be seen from the micrographs that the particle size increases from (A) to (D) and all the samples contain a percentage of sub-micrometre particles.

Table 2 shows the specific surface area and total pore area obtained using a Micromeritics Gemini 2375 (N_2 BET) and a Micromeritics Autopore III (mercury intrusion porosity).

The porosity or pore size distribution was measured using a Micromeritics Autopore III. The data are represented in Fig. 6(A)–(D) for the four different powders. Plots (A) and (B) show Zircon 1a and Zircon 2b and (C) and (D) show Zircon 3c and Zircon 4d. Since a wide range of pore sizes is measured, it is convenient to present the pore diameter on a logarithmic scale as the abscissa and log differential intrusion ($\delta V/\delta(\log D)$) (the rate of change in pore volume with change in the log of pore diameter), as the ordinate.

The plots for Zircon 1a, Zircon 2b and Zircon 3c show binodal character. The first peak corresponding to approximately 0.25 μm is sharp. The second, at approximately 60 μm is broad. The sharp peak is probably due to
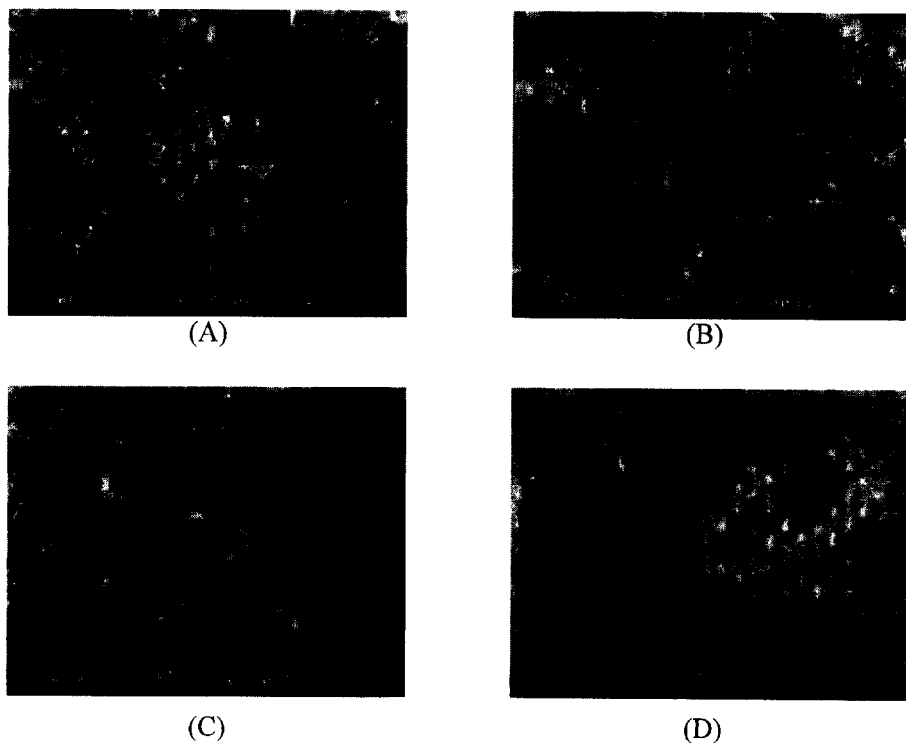

(A)

(B)

(C)

(D)

Fig. 5. SEM micrographs.

mercury penetration of pores and entry into the particle–particle voids. The broad peak is probably due to mercury intrusion within the spacial regions between clusters of particles, i.e. strong agglomerates. The plot for Zircon 4d shows only a broad peak corresponding to approximately 2 μm; this shows probable penetration of pores and entry into the particle–particle voids only, which is due to the coarseness of the particles.

Table 3 shows the values calculated from heats of immersion measurements. Blank readings were measured and subtracted from the heats of immersion measurements. All the values are averages, taken from a minimum of six measurements. The deviation about the mean is in the range 0.3–4%.
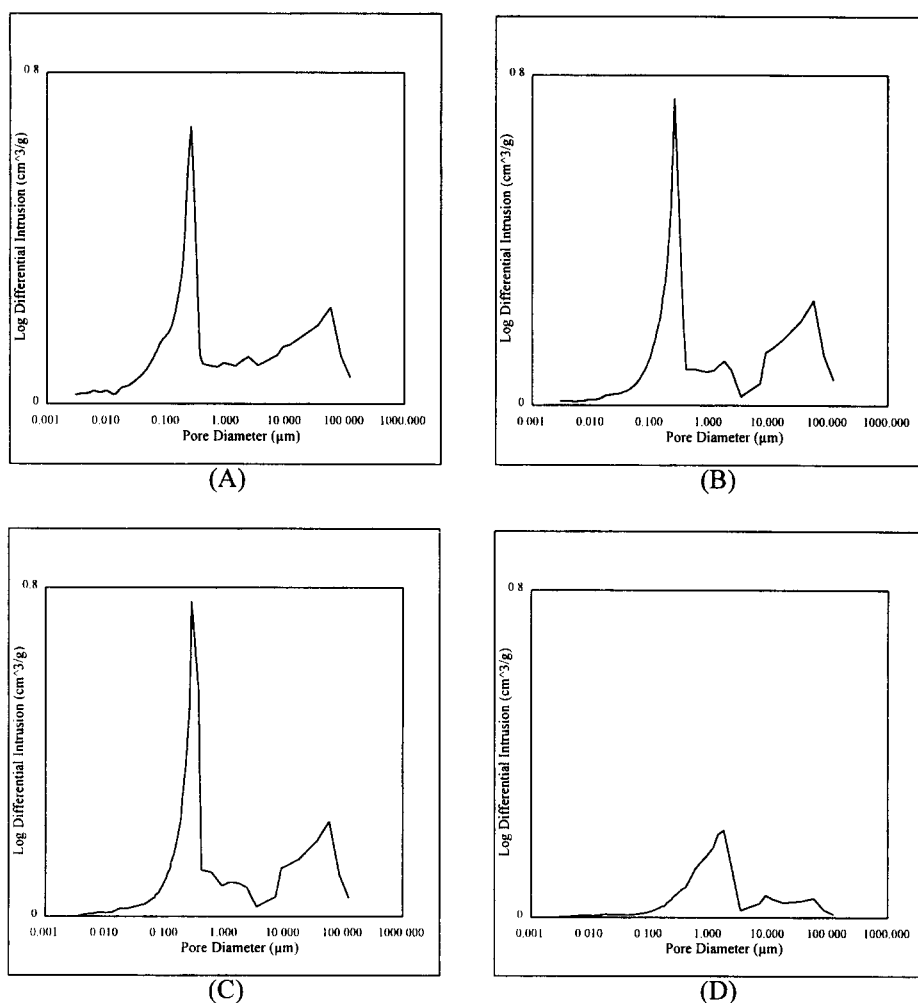

Fig. 6. Pore size distribution, Micromeritics Autopore III.

The heats of immersion values were measured at 20°C. The time taken for evolution of the heat during immersion did not exceed 3–5 min. This is in accordance with the findings of several other authors [14–20].

Figure 7 shows the particle D_{50} (volume median value) as a function of the heat of immersion. Here Fig. 7(A) and (B) show the measurements obtained by the Malvern Mastersizer and the Coulter Counter, respectively. From the plots (Fig. 7) it can be seen that the values obtained for the heats of immersion, increase with an increase in the fineness of the powder, with the
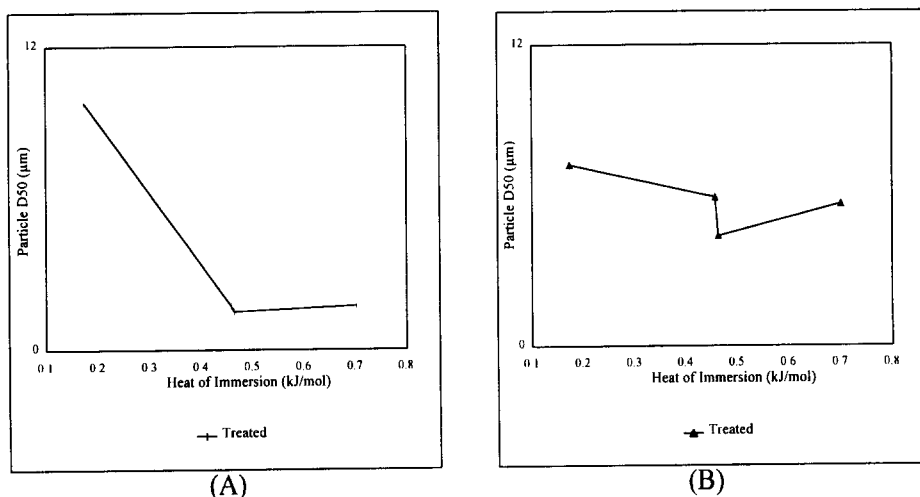

(A)   (B)

Fig. 7. Particle D_{50} as a function of $\partial H_{\text{immersion}}$.

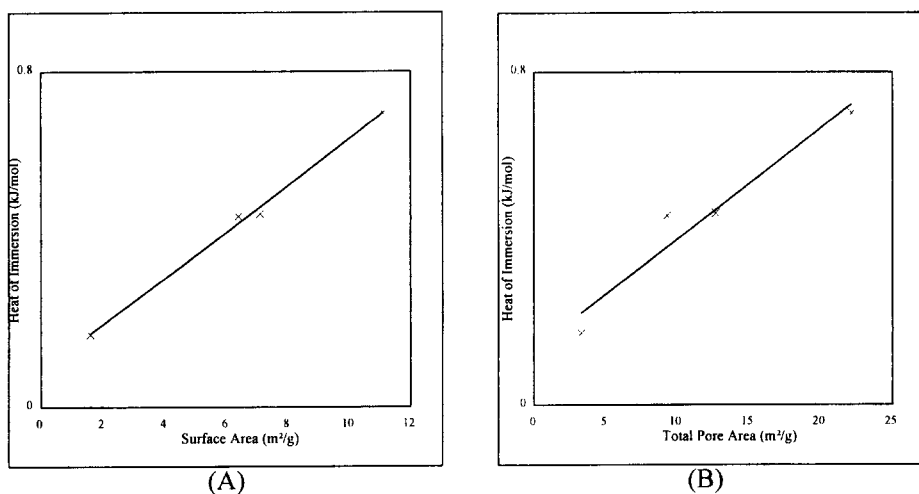(A)   (B)

Fig. 8. Area as a function of $\partial H_{\text{immersion}}$.

exception of Zircon 1a. This value probably arises as a consequence of agglomeration as shown by the distinctive binodal distribution in Fig. 4 and also in the SEM micrographs (Fig. 5).

Since only the D_{50} values are given by the particle size analysers, it is more meaningful for the heats of immersion to be expressed in terms of the surface area of the powder.

Figure 8 shows the specific surface area (A) and the total pore area (B) as a function of the heats of immersion. From these plots it can be seen that as the area of the powder increases, the value of the heat of immersion increases.

CONCLUSIONS

Two units have been built and designed. The first was a high vacuum system used to clean/degas the powder surface. The second was an immersion unit, used in the evaluation of the heats of immersion. This unit was finely tuned and gave a maximum error of 4%.

A comprehensive approach to the determination of the surface characteristics of zircon powders has been described and demonstrated. Such studies are important because of their implications for ease of dispersion and for the stability of the dispersion so generated.

REFERENCES

1. Cookson Matthey Ceramics and Minerals Ltd, *Cookson Matthey material data sheet*, Cookson Matthey Ceramics and Minerals Ltd, Tyne & Wear, UK, 1993.
2. Zettlemoyer, A. C., *The Interface Symposium*, 7 (1965) 27.
3. Bartell, I. E. and Suggit, R. M., *Journal of Physics and Chemistry*, 58 (1954) 36.
4. Boyd, G. E. and Harkins, W. D., *Journal of the American Chemical Society*, 84 (1942) 1190.
5. Chessick, J. J. and Zettlemoyer, A. C., *Advances in Catalysis*, 2 (1959) 263.
6. Hutchinson, E., *Transactions of the Faraday Society*, 43 (1946) 443.
7. Sillars, J., *Instrumentation*, 19 (1942) 81.
8. Zettlemoyer, A. C., Young, G. J., Chessick, J. J. and Healey, F. H., *Journal of Physics and Chemistry*, 57 (1953) 649.
9. Pierce, W. C., Mooi, J. and Harris, R. E., *Journal of Physics and Chemistry*, 58 (1958) 36.
10. Hutchinson, E. and Manchester, K. E., *Review of Scientific Instruments*, 26 (1955) 364.
11. Kiselev, A. V., Kiselev, V. F., Mikos, N. N., Muttick, G. G., Runov, A. D. and Shcherbakova, K. D., *Journal of Physics and Chemistry (U.S.S.R.)*, 23 (1949) 577.
12. Winslow, D. N., *Surface and Colloid Science*, 13 (1984) 259.

13. Clyde, O., Jr, *Powder Technology*, **3** (1969) 70.
14. Egorov, M. M., Kiselev, V. F., Krasilnikov, K. G. and Murina, V. V., *Zhurnal Fizicheskoi Khimi*, **33** (1959) 65.
15. Makrides, A. C. and Hakerman, N., *Journal of Physics and Chemistry*, **63** (1959) 594.
16. Tyler, A. J., Taylor, J. A. G., Pethica, B. A. and Hockey, I. A., *Transactions of the Faraday Society*, **67** (1971) 483.
17. Egorov, M. M. and Kiselev, V. F., *Zh. Fiz. Khim.*, **36** (1962) 318.
18. Partyka, S., Rouquerol, I. and Rouquerol, J., *Journal of Colloid and Interface Science*, **68** (1979) 21.
19. Griffiths, D. A. and Fuerstenau, D. W., *Journal of Colloid and Interface Science*, **80** (1981) 271.
20. Milonjic, S. K., *Thermochimica Acta*, **78** (1984) 341.